Long-Range Channel Measurements on Small Terminal Antennas Using Optics

Yanakiev, Boyan; Nielsen, Jesper Ødum; Christensen, Morten; Pedersen, Gert Frølund

Published in:
I E E E Transactions on Instrumentation and Measurement

DOI (link to publication from Publisher):
10.1109/TIM.2012.2196391

Publication date:
2012

Document Version
Early version, also known as pre-print

DOI: 10.1109/TIM.2012.2196391

URL: http://ieeexplore.ieee.org/xpl/login.jsp?tp=&arnumber=6220880

Boyan Yanakiev
Lindholm Brygge 35
9400 Nørresundby
Denmark
Phone: +45 60699017
Fax: +45 98151564
Email: boyany@gmail.com

Long Range Channel Measurements on Small Terminal Antennas Using Optics

Boyan Yanakiev, Jesper Ødum Nielsen, Morten Christensen and Gert Frølund Pedersen

***Abstract*—In this paper details are given on a novel measurement device for radio propagation channel measurements. To avoid measurement errors due to the conductive cables on small terminal antennas, as well as to improve the handling of the prototypes under investigation, an optical measurement device has been developed. It utilizes thin, light and flexible glass fibers as opposed to a heavy, stiff and conductive coaxial cables. The paper looks at the various system parameters such as overall gain, noise figure and dynamic range and compares the solution to other methods. An estimate of the device accuracy is also given. Selected parts of the circuitry are given in more details. Typical measurement results are also shown.**

***Index Terms*—optical fiber, propagation measurements, optical fiber measurement applications, antenna, MIMO systems, electrically small antennas, handset antennas**

I. Introduction

MOST up-to-date and future communication standards (WiMax, LTE, LTE-A, 802.11n) include some type of Multiple Input - Multiple Output (MIMO) scheme with the purpose of boosting the overall throughput in the system. Many of these standards also include small, mobile phone size, device categories [1], where the antenna design is in general challenging due to the fundamental limitations of antennas [2], [3]. It is also known that if the antenna can be identified as electrically small, measurement cable effects become a significant source of errors in nearly all types of antenna measurements, [4]–[7]. The additional antennas required for the MIMO schemes, pose even further challenges to the design as well as performance evaluation. The already scarce space for leading out measurement cables, becomes even less and new problems arise due to the cables (one for each antenna), for example changes in coupling. Removing such measurement errors brings the antenna design closer to reality, which can be very beneficial at the early design stage.

Typical antenna measurements, which can be improved with the use of optical fiber are radiation pattern measurements, Over The Air (OTA) system measurements or propagation channel measurements. These pose different challenges that are difficult to meet with one solution. Also, it is desirable that a solution is flexible in terms of carrier frequency, can accommodate high bandwidth and is easy to handle and mechanically robust.

B. Yanakiev and M. Christensen are with Molex Antenna Business Unit in Aalborg, Denmark .

B. Yanakiev (postdoctoral researcher), J. Ø. Nielsen and G. F. Pedersen are with the Antennas, Propagation and Radio Networking section at the Department of Electronic Systems, Faculty of Engineering and Science, Aalborg University, Denmark

B. Yanakiev and J. Ø. Nielsen are sponsored by the Danish Advanced Technology Foundation (Højteknologifonden) as part of the Converged Advanced Mobile Media Platform (CAMMP) project.

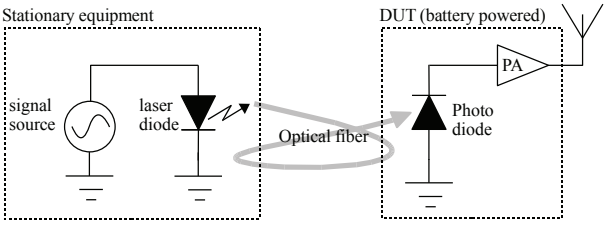

Fig. 1. Block diagram of an optical link solution for low power output. The amplifier (PA) may not be needed.

In the case of low propagation loss between the Transmitter (TX) and the Receiver (RX), only relatively low power needs to be emitted by the TX to give sufficient power at the RX side. This would typically be the case for radiation pattern measurements or propagation measurements at short distances. Fig. 1 shows a block diagram of a typical optical solution suitable for the low channel loss scenario. The output of an optical detector diode can often be used directly, without additional amplification. For typical optical power levels around 3-10 dBm, the current is 3-6 mA. The RF output power is about 0 dBm and the device can be used from about 100 MHz to about 6 GHz, depending on the components selected, all commercially available. In the example of Fig. 2 an Emcore [8] detector diode is used. The block size is about $20 \times 17 \times 10$ mm and integrated as part of the radiating structure of a small Planar Inverted F Antenna (PIFA) antenna. The detector requires an external power source but since the consumption is low, a single cell battery is sufficient for several hours of operation. Attention has to be paid to the battery maximum continuous current drain specifications to ensure the linearity of the link. The other end of the optical fiber is connected to a laser. Since this unit would be located together with the stationary equipment, the size and power consumption are not critical. Thus, an off-the-shelf laser can be used. An even better solution is available to manufacturers; the detector diode inside the unit is actually very small, about 1 mm in diameter, and hence could easily be integrated into, e.g., an SubMiniature version A (SMA) connector. This type of solution is popular in literature when optical pattern measurements are needed - [9], [10].

This paper looks at an alternative type of optical measurement device for long range propagation channel measurements, for example in urban environments. Most of the developments in the area are either too big [10], [11], short range [9], [10], [12] or suitable for anechoic chamber only. The

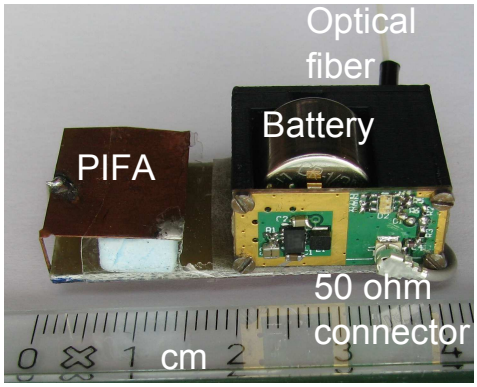

Fig. 2. Example of a PIFA antenna with an optical link device for low power transmission. The scale is in cm.

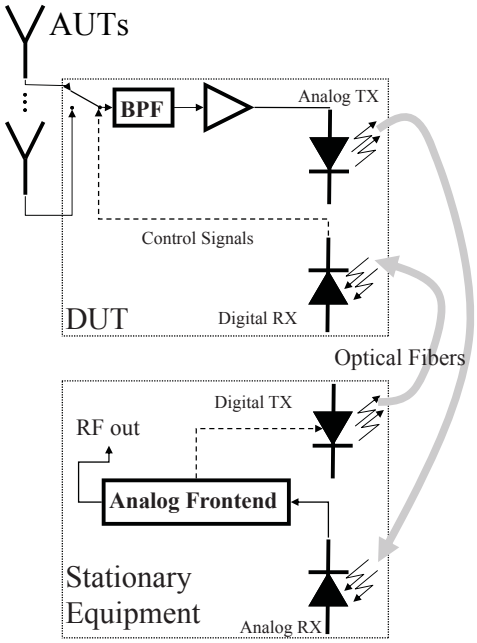

Fig. 3. Block diagram of a battery driven receiving DUT with optical output.

device presented here is specifically designed to fit in a small volume and is optimized for low power consumption, thus imitating the phone electronics. It can be used in an anechoic or reverberation chambers, however it is best suited for long range channel sounding. The paper gives further details and supports the work presented in [13] and [14].

Using the channel reciprocity, the high power needed for long range applications, can be at the stationary equipment side and the Device Under Test (DUT) is then a receiver. Fitting a linear, analog laser in small volume however is not easy. The insertion loss is rather high, increasing the noise dramatically unless the signal is pre-amplified. However, adding the needed about 20 dB of gain inside a small DUT can lead to oscillations due to signals coupling back into the Antenna Under Test (AUT). Furthermore, a number of filters would be needed, to ensure the device's compatibility with systems such as Global System for Mobile communication (GSM) already operating in the area, where the sounding is to be performed. All this adds to the size and complexity of the circuit. Fig. 3 shows a block diagram of the realized circuit, where it is noted that multiple antennas can be included by switching.

Despite the increased complexity of the RX optical solution, there can be major advantages when long range channel sounding is needed. For example, the measurements described in [15], [16] include two separate Base Stations (BSs) with multiple transmitters on each and large separation (several hundred meters) in urban environment. In a typical correlation sounder, the receiver is usually much more complex and expensive than the transmitter, making the split to receiving base stations undesirable. Also, synchronization over multiple kilometers becomes an issue when truly simultaneous channel sounding is required. Alternatively, if the base stations are transmitting, the much simpler and cheaper transmitter needs to be split. In addition the range of the sounding can be easily extended by adding additional amplification at the stationary equipment side. Note that additional 20 dB amplification on a battery powered mobile handset can be an issue.

The RX optical device in this paper addresses a channel sounding scenario with multiple BSs and high propagation channel loss conditions. The fully parallel architecture and simultaneous sounding allows for investigations in the area of cooperative MIMO using measurement data.

The paper is organized as follows: Section II introduces the main considerations for the optical link design followed in Section III by a description of the actual device built. Section IV looks at the device RF performance and analyzes potential sources of errors and Section V shows measurement results. Section VI concludes the paper.

II. Intrinsic Optical Link

Analog optical links at microwave frequencies are most commonly used for antenna remote operations as well as in the CAble TeleVision (CATV) sector. Most laser components on the market target those applications. Although, antenna measurements with optical links are gaining more attention, the optical components, available on the market are still limited to relatively large devices, most often with built-in cooling elements. The cooled lasers are inadequate for the application in this paper, due to the large size and about 1.5 A current consumption of the Peltier cooling element [17].

Thus un-cooled lasers must be used, which can lead to non-linearity due to temperature variation. Since the target application of the device described here is channel measurements, and those can take place both outdoor and indoor, temperature variability can be an issue. Another major size constraint is the modulator. The use of the industry standard Mach-Zehnder optical modulator is difficult, again due to the typically large size of those devices. Therefore, direct modulation is the best candidate with size being the major benefit, despite the overall worse performance in terms of any other parameter such as noise figure (NF), insertion loss etc. With the above application specific considerations in mind, the implementation of the optical antenna measurement tool follows a standard path.

All equations relating to the optical link are directly taken from [18]. The goal here is to highlight the practical considerations for the specific application described, rather than

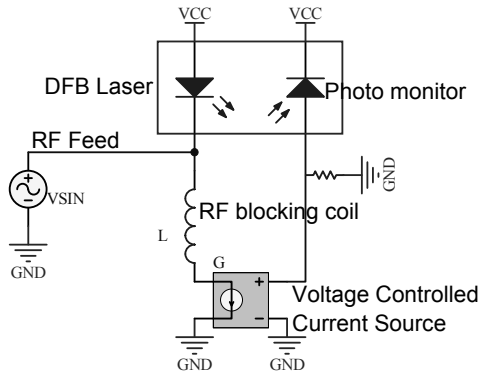

Fig. 4. Laser biasing block diagram. The RF feed is amplitude modulating the laser current around the bias point set by the current driver. Voltage feedback from the built in photo-monitor moves the biasing point, according to the temperature related optical power variation and stabilizes it around the desired level.

improve on existing optical link technologies. Following the definition in [18], the link including the optical modulator, bias circuit and detector is called intrinsic. The device parameters, including the switching, filter blocks and pre-amplification stage are called Optical Unit (OU) parameters.

All results presented here are obtained by using an off-the-shelf detector diode from Discovery Semiconductors (DSC50) in the other end of the link.

A. Laser bias

Fig. 4 shows the basic laser biasing schematic of the OU. A current driver, implemented with a precision operational amplifier [19], provides the basic laser DC operating point at about 15 mA. This is according to what most manufacturers give as the best DC bias point following

$$I_{op} = I_{th} + 10\ [mA] \tag{1}$$

where I_{op} is the operating current and $I_{th} = 5$ mA is the laser diode threshold current. Due to the very low power operational amplifier ($I_{SY} < 1$ μA [19]) the total current consumption of the block is effectively equal to the current in the laser. The output optical power in this case, is around 3 dBm. Temperature stabilization is implemented utilizing the built in photo monitor and providing control voltage feedback to the current driver. All values given are typical based on a high efficiency Emcore laser diode [20].

It can be seen from Fig. 4 that the input impedance as seen from the RF part will not necessarily be 50 ohm. Therefore a series resistor is needed for matching. This way of direct modulation leads to the high insertion loss of the circuit.

B. Intrinsic link gain - G_{intr}

Despite the name it has been shown [21] that, it is hard to achieve actual positive gain in direct modulation intrinsic links. In this case the measured gain is around -14 dB depending on frequency. A simple theoretical formula is given in [18] $G_{intr} = s_l^2 r_d^2 = -13.6$ dB, where $s_l = 0.30$ W/A is the laser slope efficiency and $r_d = 0.7$ A/W is the detector responsivity, with their typical values. The formula assumes perfect match between input and output impedances. These parameters however can vary significantly from one laser to another.

C. Intrinsic link Noise Figure (NF) - NF_{intr}

When calculating the system NF using Friis' cascade equation, it is worth noting that for optical links, the NF is not simply the reciprocal of the loss as in attenuators for example. Additional noise sources such as the laser Relative Intensity Noise (RIN) and the detector shot noise, contribute to the total noise in the overall intrinsic link. When direct modulation is used the RIN noise is assumed dominant and calculated according to [18]

$$NF_{intr} = 10\lg\left(2 + \frac{(I_D^2 10^{\frac{RIN}{10}} R_{LOAD})}{2 s_l^2 r_d^2 kT}\right) \approx 26.4\ [dB] \tag{2}$$

where $I_D = OP \times r_d$ is the detector current, $RIN = -150$ dB/Hz is the RIN from the laser specifications in dB/Hz, $R_{LOAD} = 50$ ohm is the loading impedance, $OP = 2$ mW is the delivered optical power, k is the Boltzmann constant and finally $T = 293$ K is the absolute temperature. All values given are typical.

For the device presented here the measured NF is about 28-30 dB depending on frequency. From a practical point of view such high noise figure is hard to measure and only the gain method [22] gives adequate results.

D. Intrinsic link Dynamic Range (DR) - $IMF_{3,intr}$

The dynamic range is also an important parameter especially when the goal is to characterize fast fading mobile channels. Again [18] provides a simple engineering formula $IMF_{3,intr} = 2/3(IP_{3,intr} - (G_{intr} + NF_{intr} + kT\Delta f)) = 58$ dB, for the inter-modulation free dynamic range of the intrinsic link, where IP_3 is the third order intercept point and Δf is the bandwidth. All parameters are in dB or dBW. The calculation is made for a 40 MHz bandwidth and computed third order intercept point of $IP_{3,intr} = -27.6$ dBW.

III. Proposed OU

The high NF and insertion loss require a pre-amplification block feeding the laser. The complete device proposed here consists of the following major components:

- Laser bias and modulator (essentially a part of the intrinsic optical link discussed in Section II)
- RF amplification block
- DC-DC step-up converter for battery power supply
- Control block for antenna switching

Fig. 5 shows the complete optical unit (OU) integrated into a 100x40 mm phone mock-up with two PIFA antennas. Only the bottom cover is shown in the photo. The small device size allows for the complete OU to be integrated within the radiating structure, which includes the entire mock-up length at the lower GSM bands.

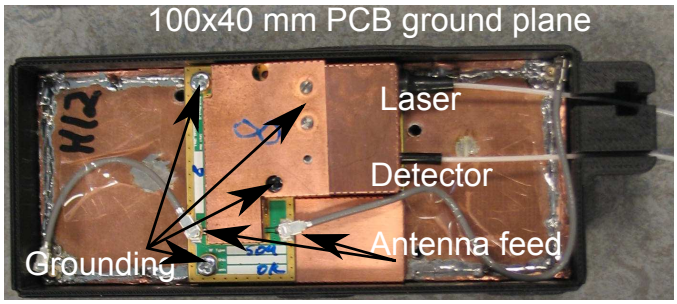

a) Top view

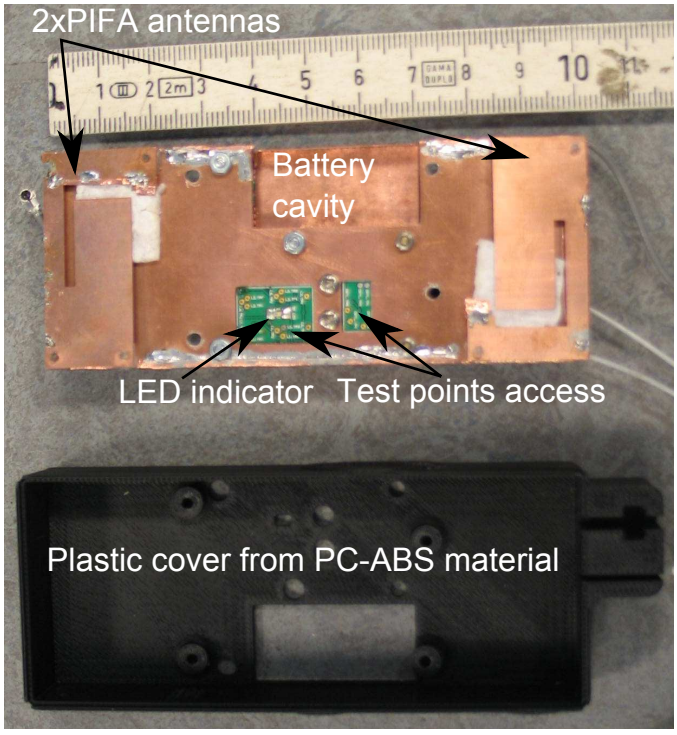

b) Bottom view

Fig. 5. Realized optical unit integrated into a 100x40 mm phone mock-up. The total OU size is $40x40x10$ mm including the battery cavity. Microcoaxial connections are used to minimize size [23].

A. RF amplification block

Fig. 6 shows a block diagram of the RF circuit, based on a single Avago chip [24]. RF filters are needed to select the operating band of the device to avoid saturation by unwanted signals. For the purposes of a large scale measurement campaign conducted in Aalborg, Denmark in May 2011, two frequency bands have been selected - one low and one high, centered at 796 and 2350 MHz and with bandwidths of 20 and 100 MHz respectively. The filter block therefore consists of two commercially available filters in parallel. The filters used are not specifically designed for the working frequencies but a practical trade off was made between filter availability and interferers present at the measurement site - GSM900 and DVB-T on the low band and UMTS/WLAN base stations on the high band.

The antenna switching is implemented with a Hittite [25] high isolation switch, providing around 65 dB of measured

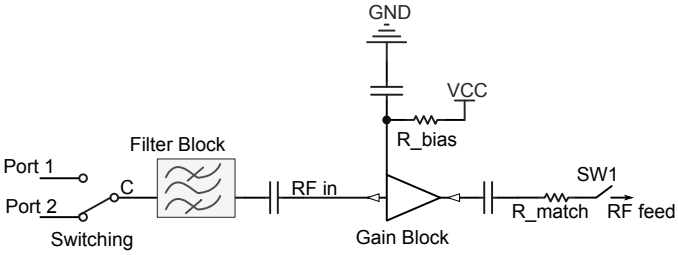

Fig. 6. RF block diagram. The bandpass filter block actually consists of two commercially available filters in parallel.

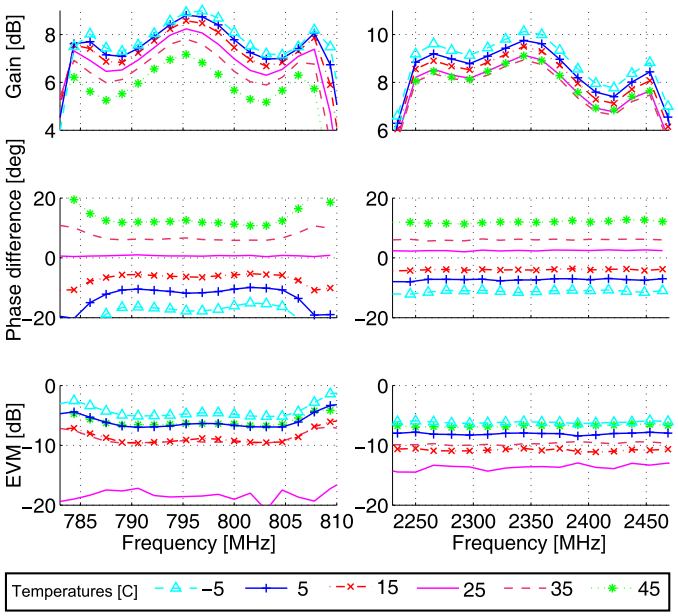

Fig. 7. Temperature dependency of the Optical Unit. The phase and EVM difference plots are referenced to the first 25 degrees measurement.

port isolation for the PCB layout used.

B. OU RF link gain - G_{OU}

Since temperature variation can be a problem, the system link gain was measured across temperatures sweeping up and down to verify to what extend the optical unit remains stable as well as check the repeatability of the measurements - Fig. 7. The phase and Error Vector Magnitude (EVM) plots are referencing an initial 25 degrees measurement. The repeated measurements for each temperature lie practically on top of each other with EVM lower than -15 dB in all cases. For figure readability only one repeated case is shown for the 25 degrees on the phase and EVM plots. The repeated measurements were taken across several days in a climate chamber.

The maximum gain variation due to temperature is a bit over 2 dB from the lowest to the highest temperatures. As can be expected the high temperatures result in lower gain. In general, for a realistic variation of about 30 degrees, the temperature variation is within 0.8 dB. As an improvement of the optical unit, a temperature sensor can be implemented to record the instantaneous ambient temperature and include this information into the calibration procedure.

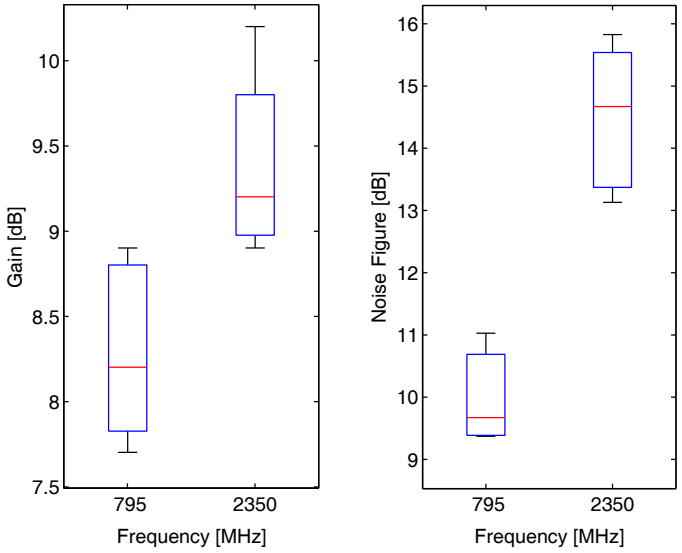

Fig. 8. Gain and NF statistics for selected frequencies and for all temperatures listed in Fig. 7. See [26] for interpretation.

TABLE I
OU PARAMETERS

Parameter	Symbol / Units	Values	
		796 $[MHz]$	2350 $[MHz]$
Intrinsic Link Gain	G_{intr} $[dB]$	-13	-15
Intrinsic Link NF	NF_{intr} $[dB]$	25.8	27.8
Intrinsic Link DR	$IMF_{3,intr}$ $[dB]^*$	58.3† / 55.6$^\triangleleft$	
OU Gain	G_{OU} $[dB]$	8.2	9.2
OU Noise Figure	NF_{OU} $[dB]$	9.7	14.7
OU Noise Floor	$P_{N,OU}$ $[dBm/Hz]$	-156	-150
OU IP3	$IP_{3,OU}$ $[dBm]$	2	1
OU Dynamic Range	$IMF_{3,OU}$ $[dB]$	55 †	47 $^\triangleleft$
Port Isolation	Iso $[dB]$	61	65
Current Consumption	I_q $[mA]$	80	
Battery Life	$-$ $[min]$	60	
Supply Voltage	V_{batt} $[V]$	3.7	
Optical Power	OP $[dBm]$	3	

* Computed rather than measured values
† Computed for 40 MHz bandwidth
$^\triangleleft$ Computed for 100 MHz bandwidth

C. OU Noise Figure - NF_{OU}

The measured NF at room temperature, of the complete optical unit is between 9 and 14 dB depending on frequency. Fig. 8 shows simple box-plot statistics of the measured gain (left) and noise figure (right) for the same temperatures as in Fig. 7. The box central line is the sample median and the lower and upper box boundaries are the 25 and 75 percentiles respectively. For more details, see the *boxplot* function of Matlab [26]. Overall the temperature variation of the noise figure falls within the measurement accuracy of the method used.

Since this NF is rather big, it is interesting to compare it to an alternative solution. Common practice when measuring propagation channels is to simply connect the antenna to the sounding equipment with conductive RF cables. In that case no gain blocks, immediately after the antenna would be added, thus making the comparison unfair but still realistic from a practical point of view. Under the assumption that the sounding equipment is about 15 meters away to allow for free movement during measurements, the corresponding cable loss and therefore NF, can be easily calculated. For a high quality, low loss, phase stable cable [27] (usually in use at Aalborg University) the specified loss is 0.2 dB/m at 1 GHz. Therefore for a length of 15 meters some 3 dB of losses will be added. The figures presented for the optical link are for 20 meters optical fiber but the difference is negligible up to few km. Even in this unfair comparison a cabled solution shows better results. It must be considered however, that the cables in question are rather stiff and very uncomfortable for use, if users are involved, and especially if natural phone handling is desired. Of course previously mentioned considerations regarding measurement errors due to radiation from the cables also apply.

D. OU Dynamic Range - $IMF_{3,OU}$

The third order intercept point of the RF block is $IP_{3,RF} = 15$ dBm, [24]. The result is measured $IP_{3,OU} = 2/1$ dBm, depending on frequency. The inter-modulation free dynamic range of the complete OU is then calculated to be $IMF_{3,OU} = 55/47$ dB for 40/100 MHz bandwidth respectively. This is sufficient for both channel sounding and radiation pattern measurements. Since the OU does not include an on board Automated Gain Control (AGC) it is effectively the limiting factor in wide band channel measurements since most channel sounders have wider DR. The optical DR however can still accommodate 10-15 dB of user attenuation and some 30 dB of Rayleigh fading - see Section V-B

E. Control block

The digital control circuit is used for switching between up to two antenna inputs. The optical link is implemented with single mode fiber and the major concern has been the switching speed. The combined switching and measurement time for all antennas, should be lower than the channel coherence time to ensure quasi-static conditions. This is essential if parameters such as correlation or capacity are to be computed from the complex channel impulse response. For urban environments and low speeds, the coherence time is about $T_c \approx 100$ ms. With this in mind, the switching time achieved of about $T_{switch} \approx 100$ ns is more than sufficient. The switching circuit is a simple transimpedance amplifier followed by a comparator. In case more than two antennas need be supported, a counter can be included combined with a different RF switch.

Power for the OU is drawn from a single cell *LiIo* rechargeable battery with dimensions $25x20x5$ mm. The nominal output from the battery is $V_{batt} = 3.7$ V with about 130 mAh capacity. The measured third order harmonics from the DC-DC converter are below -68 dBc. Table I gives a summary on the parameters discussed so far.

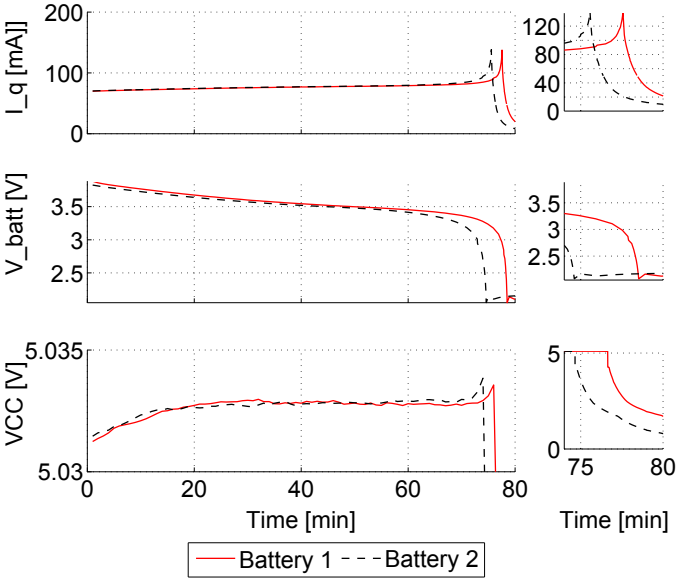

Fig. 9. DC-DC output voltage vs. battery depletion for two batteries.

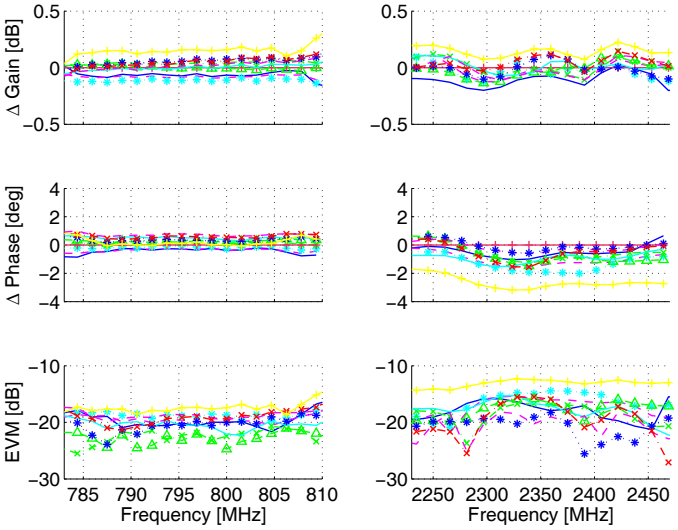

Fig. 10. Variation introduced by fiber movement - multiple measurements shown.

IV. Sources of Errors and Linearity

Multiple sources of errors are possible in a measurement system utilizing such OU. The ones related to the OU itself and optical fibers are analyzed here.

A. Battery influence

Temperature variation contributes to less than 10 mV supply voltage change and is already included in the variation from Fig. 7. Another potential source of uncertainty is the slow degradation of battery output voltage over usage time. As the battery is being depleted however, no significant supply voltage change was experienced. At the battery limit, the DC-DC converter simply shuts down. A simple LED was used for indication of proper operation and to avoid operator mistakes. The maximum usage time with the battery from Section III and at $I_q \approx 80$ mA total power consumption, is about 70 minutes. A conservative estimate is about one hour. Fig. 9 shows two batteries being depleted over time and the corresponding current consumption I_q (top), battery voltage V_{batt} (middle) and DC-DC voltage output V_{cc} (bottom). Notice that the scale range on the bottom plot is only about 5 mV and the total change is around 3 mV. These values are not significant for the laser bias or the RF gain blocks.

B. Influence of the optical fiber connections

It is interesting to estimate the uncertainty introduced by the optical fibers and the corresponding connections. To do that, the following simple tests were performed:

1) Bending the fiber under various angles: this can result in optical power loss and phase change. According to [28] the minimum bend radius allowed without optical losses, is around 1-2 inches (25-50 mm), depending on fiber type and usage conditions. These are however static characteristics and it is interesting to see if the dynamic movement of the fiber during measurement can contribute to any significant variation. To verify this, 11 measurements were performed with a VNA recording the complete link response, while a person was randomly moving and bending the fiber, not violating the minimum radius condition. The resulting Error Vector Magnitude (EVM) (computed relative to an initial static reference measurement) is always below -15 dB (3%) for the low band and -10 dB (10%) for the high band - Fig. 10. This error can be minimized with proper care of the mechanical movement of the fiber during measurement.

2) Multiple connect/disconnect cycles: In this case, the primary concerns are optical reflections and dirty fibers. For the SC connector used in this case, reference data is given in [29]. EVM of up to -8 dB was observed compared to an initial reference measurement, without any special care taken between connections, indicating that this could be an issue. Practical experience showed however, that with proper treatment of the optical connector (cleaning and protecting from scratches), the uncertainty can be minimized to the values given in [29]. This is a necessary expenditure of time when working with optical connectors, which are rather different from the coaxial alternative.

C. Total uncertainty of the optical link

To evaluate the total uncertainty [30] in the optical link the following approximate values are used for the corresponding uncertainty sources:

- Uncertainty due to temperature change within realistic 20-30 degrees range - ± 0.4 dB (type B) - $u = \frac{0.4}{\sqrt{(3)}} = 0.23$ dB assuming uniform distribution
- Uncertainty due to battery drain over time before cut-off - ± 0.05 dB (type B) - $u = \frac{0.05}{\sqrt{(3)}} = 0.03$ dB assuming uniform distribution
- Uncertainty due to optical interconnections (type A) - $u = \frac{0.19}{\sqrt{(5)}} = 0.08$ dB assuming normal distribution for 5 repeated measurements

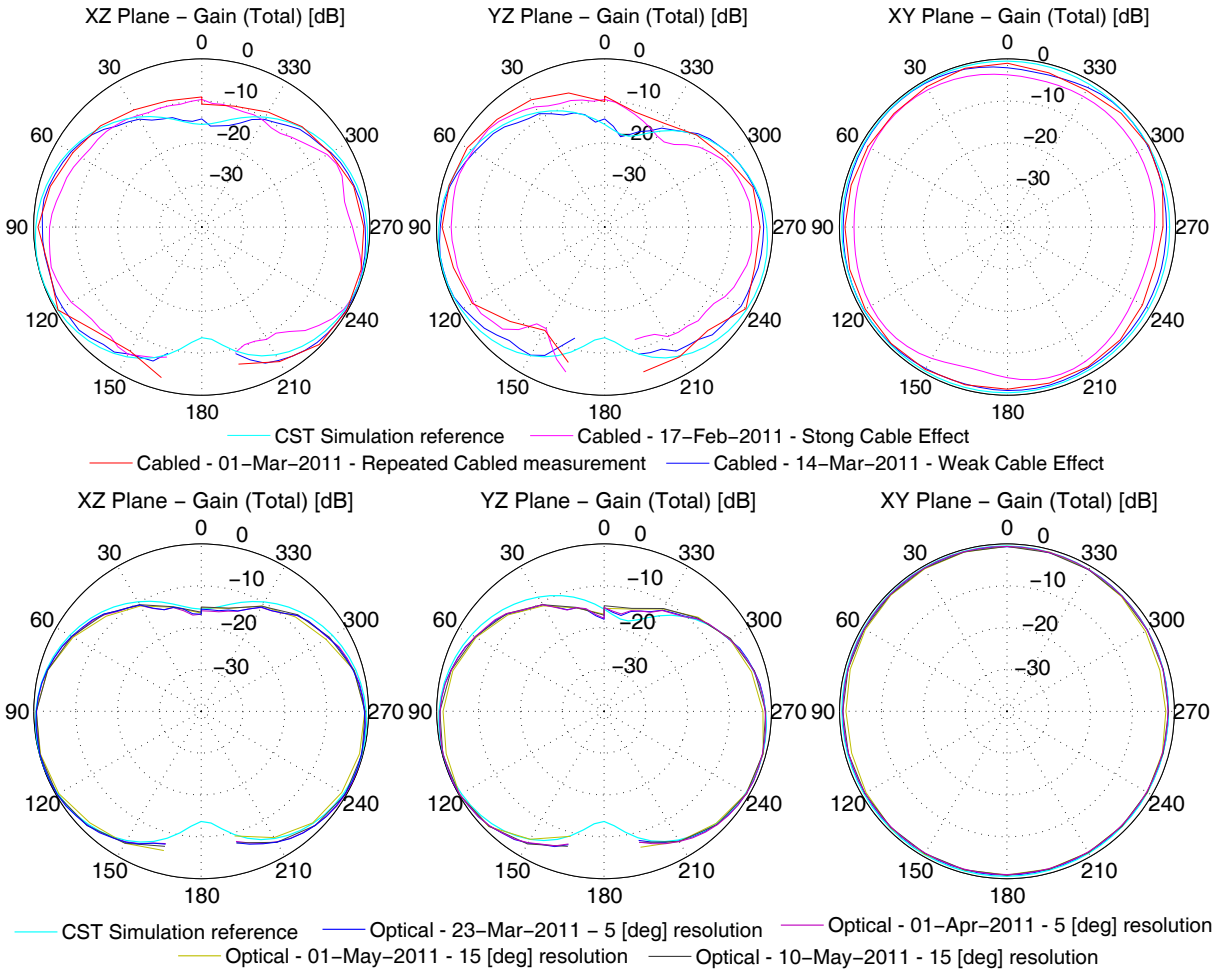

Fig. 11. Multiple 796 MHz radiation pattern measurements with cables (top three) and with optics (bottom three). The discontinuity at $\theta = 0$ is due to misalignment when positioning the mock-up.

- Uncertainty due to fiber movement (type A) - $u = \frac{0.19}{\sqrt{(11)}} = 0.03$ dB assuming normal distribution for 11 repeated measurements

The combined uncertainty for two optical connections is $u_c = 0.26$ dB. Finally the expanded uncertainty with k factor of 2 (95%) is ± 0.53 dB. For the target application of channel sounding this is well below the expected channel variations, therefore acceptable. The short range solution can have better accuracy due the possibility of using cooled lasers and static fibers. It must be noted that other sources of uncertainty within the complete measurement set-up are not included in the estimate above. Also the uncertainty mentioned here is related only to the gain of the optical link and does not contribute to changes in the directivity pattern.

V. Measurement Verification

To verify the proposed device two types of measurements are presented - controlled, anechoic chamber pattern measurements and outdoor-to-indoor long range channel sounding measurements. The goal of the first one is to demonstrate the benefits of the optical fiber connection in terms of pattern accuracy and overall systems stability and repeatability. The propagation measurements presented here should be seen as confirmation of the sufficient dynamic range, speed and signal quality the device provides.

A. Anechoic Chamber Measurements

Figure 11 shows the radiation pattern of the same antenna measured multiple times with cables (top three plots) and again with the OU proposed here (bottom three). In both cases the reference is the simulated pattern. The antenna measured is one of two antennas integrated in a 111x59 mm size mock-up, similar to the one shown in Fig. 5. In the case of cabled measurements, the cables were lead out from the handset along the width of the mock-up and choked with ferrite beads. The dates of the measurements are indicated to demonstrate the long term repeatability of the optical measurements.

To quantify the differences the correlation between the measurements was computed for the isotropic environment as defined in [31]. Since all patterns are of the same antenna ideally the correlation should be always $\rho = 1$. Due to inaccuracies, however this is not the case. In the case of cabled measurements, the correlation is between 0.76 and 0.83 depending on, which two patterns are being used for the computation. In the case of the optically measured patterns the correlation is between 0.95 and 0.99. Similar is true for

multiple measurements on the second antenna of the mock-up.

When computing the correlation between the two different antennas of the handset, Fig. 12 is produced. The prefixes C and O indicate cabled and optical measurements, respectively. The 5 and 15 degrees refer to both θ and ϕ angular stepping angles during the particular measurement, indicating that the metric is rather robust. It can be clearly seen that the cabled measurements produce very randomized and erroneous results, while the optical measurements have high degree of accuracy and repeatability. Similar conclusions can be extended to any antenna parameter taking into account the shape of the radiation pattern and the incoming power distribution as shown in [32].

It is worth noting that, while the accuracy of the shape of the radiation pattern is significantly better using optics, the antenna total efficiency accuracy is typically sacrificed, with the uncertainties described in Section IV being higher than the coaxial cable alternative. However this is only true assuming the cable itself does not radiate, and ignoring for example losses in the used ferrite beads.

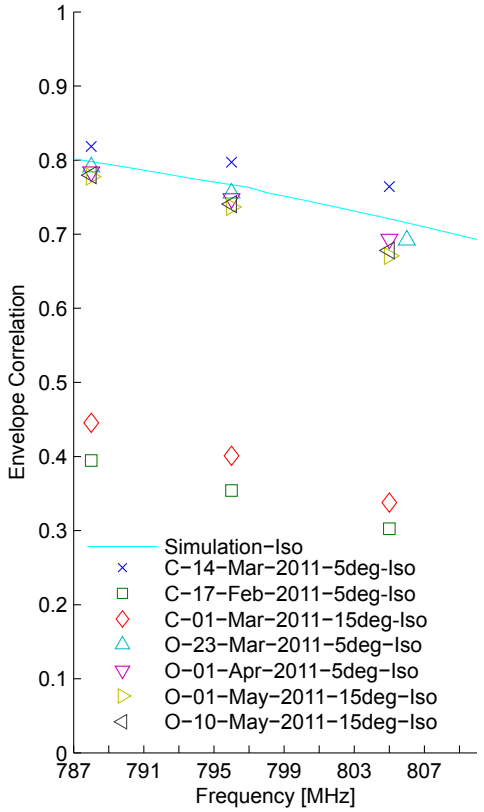

Fig. 12. Isotropic envelope correlation coefficient computed from multiple pattern measurements of a 111x59 mm dual antenna mock-up. The prefixes C and O indicate patterns measured with cables and optically, respectively.

B. Long Range Channel Sounding

Figure 13 shows an example Power Delay Profile (PDP) measured simultaneously for four different transmitters at the antenna from Fig. 11. The PDP has about 30 dB of DR, which is typically sufficient for most computations. The repeatability of the mean received power is investigated in [16] and found to

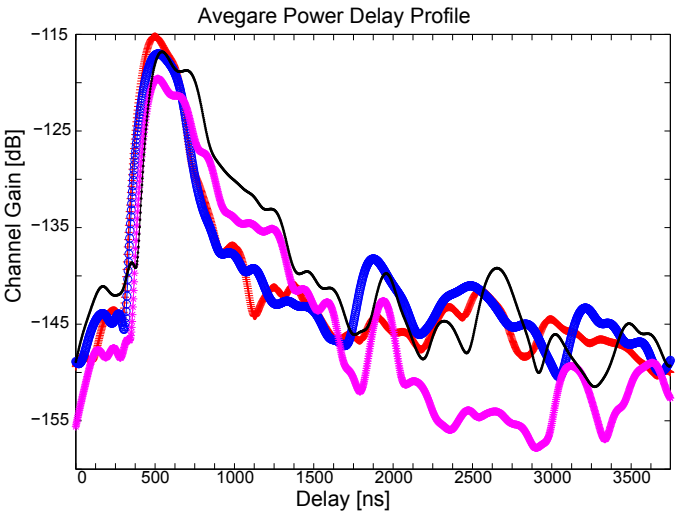

Fig. 13. Average PDP simultaneously recorded from four different transmitters.

be at most 1.4 dB, across multiple days of measurements. The 95% percentile is comparable to the optical device uncertainty discussed in Section IV-C.

The biggest advantage in using such feeding method is the preservation of the actual radiation pattern. Signal parameters strongly depending on the pattern can be better predicted and measured more accurately. For example, $\rho_e^{50\%} = 0.80$ and $\rho_e^{95\%} = 0.89$ are the percentiles of the envelope correlation of the handset from Fig. 11, computed at 796 MHz from the measured impulse responses. The slight upwards shift of the values is due to the directive environment in the channel sounding set-up. Details on the channel model dependence, correlation computation, statistical analysis and the influence on capacity are given in [15]. Note that [15] and [16] use an earlier version of the optical device described here. The channel sounding scenario is however similar.

VI. Conclusion

The paper presented a practical solution for an Optical Unit, best suited for long range channel sounding measurements. Single mode, analog laser was integrated into a small device mounted on a handset mock-up, imitating the phone electronics. The received RF signals from the mock-up antennas, are converted to optical power and lead out from the handset. This non-galvanic connection allows for a realistic antenna pattern and propagation channel interaction, avoiding the known disturbances caused by conductive cables. The receive mode architecture simplifies long range channel sounding scenarios, where multiple base stations, simultaneous sounding or wide band operation could be required.

The solution is presented in detail with block diagrams, practical considerations and uncertainty estimates. It is concluded that using optical fibers for small antenna measurements can be beneficial and accurate enough. The OU has around 45-50 dB of Dynamic Range allowing for about 30 dB DR of the measured Power Delay Profile potentially including users. The estimated uncertainty of the link is ± 0.53 dB. This

type of solution is preferred when working with small phone form factors at frequencies below 1 GHz.

ACKNOWLEDGMENT

The authors would like to thank Svetoslav Gueorguiev for his insights during the optical unit development.

REFERENCES

[1] 3GPP, 3GPP, Tech. Rep., October 2010. [Online]. Available: http://www.3gpp.org/LTE

[2] H. Wheeler, "Fundamental limitations of small antennas," *Proceedings of the IRE*, vol. 35, no. 12, pp. 1479 – 1484, dec. 1947.

[3] L. J. Chu, "Physical limitations of omni-directional antennas," *Journal of Applied Physics*, vol. 19, no. 12, pp. 1163–1175, 1948. [Online]. Available: http://link.aip.org/link/?JAP/19/1163/1

[4] W. A. T. Kotterman, G. F. Pedersen, and P. Eggers, "Cable-less measurement set-up for wireless handheld terminals," in *Personal, Indoor and Mobile Radio Communications conference, PIMRC 2001*, Sep. 2001, pp. B112–B116.

[5] C. Icheln, J. Ollikainen, and P. Vainikainen, "Reducing the influence of feed cables on small antenna measurements," *Electronics Letters*, vol. 35, no. 15, pp. 1212 –1214, Jul. 1999.

[6] P. Massey and K. Boyle, "Controlling the effects of feed cable in small antenna measurements," in *Antennas and Propagation, 2003. (ICAP 2003). Twelfth International Conference on (Conf. Publ. No. 491)*, vol. 2, march-3 april 2003, pp. 561 – 564 vol.2.

[7] S. Saario, D. Thiel, J. Lu, and S. O'Keefe, "An assessment of cable radiation effects on mobile communications antenna measurements," in *Antennas and Propagation Society International Symposium, 1997. IEEE., 1997 Digest*, vol. 1, jul 1997, pp. 550 –553 vol.1.

[8] *2651A/2651E Broadband Photodiode*, Emcore Corporation, August 2011, Data Sheet. [Online]. Available: http://emcore.com/assets/fiber/2651AE_datasheet_2008.10.30.pdf

[9] I.-K. Cho, J.-I. Mun, S.-M. Kim, and J.-H. Yun, "Optical fiber link system for the antenna measurement," in *Photonics in Switching, 2009. PS '09. International Conference on*, sept. 2009, pp. 1 –2.

[10] R. Lao, W. Liang, Y.-S. Chen, and J. Tarng, "The use of electro-optical link to reduce the influence of rf cables in antenna measurement," in *Microwave, Antenna, Propagation and EMC Technologies for Wireless Communications, 2005. MAPE 2005. IEEE International Symposium on*, vol. 1, aug. 2005, pp. 427 –430 Vol. 1.

[11] N. Clow and I. Morrow, "Esa measurements using the hybrid fibre-optic reflection measurement system," in *Antennas Propagation Conference, 2009. LAPC 2009. Loughborough*, nov. 2009, pp. 793 –796.

[12] B. Yanakiev, P. Eggers, G. Pedersen, and T. Larsen, "Assessment of the Physical Interface of UHF Passive Tags for Localization," in *First International EURASIP Workshop on RFID Technology*, Vienna, Austria, September 2007, pp. 25–28.

[13] B. Yanakiev, J. Ø. Nielsen, and G. F. Pedersen, "On small antenna measurements in a realistic MIMO scenario," in *Antennas and Propagation (EuCAP), 2010 Proceedings of the Fourth European Conference on*, Apr. 2010, pp. 1 –5.

[14] B. Yanakiev, J. Nielsen, and G. Pedersen, "MIMO channel measurements using optical links on small mobile terminals," in *Antennas and Propagation Society International Symposium (APSURSI), 2010 IEEE*, Jul 2010, pp. 1 –4.

[15] B. Yanakiev, J. anddum Nielsen, M. Christensen, and G. Pedersen, "On small terminal antenna correlation and impact on MIMO channel capacity," *Antennas and Propagation, IEEE Transactions on*, vol. 60, no. 2, pp. 689 –699, feb. 2012.

[16] J. Nielsen, B. Yanakiev, I. Bonev, M. Christensen, and G. Pedersen, "User influence on MIMO channel capacity for handsets in data mode operation," *Antennas and Propagation, IEEE Transactions on*, vol. 60, no. 2, pp. 633 –643, feb. 2012.

[17] *1614W 1310 nm DFB Laser Module*, Emcore Corporation, January 2010, Data Sheet. [Online]. Available: http://www.emcore.com/assets/fiber/1614W_datasheet_2010.01.08.pdf

[18] C. H. Cox, *Analog Optical Links: theory and practice*. Cambridge University Press, 2004.

[19] *LTC6078/LTC6079*, Linear Technologies, Inc., 2010, Data Sheet. [Online]. Available: http://cds.linear.com/docs/Datasheet/60789fa.pdf

[20] *Model 1933F/R/W Coaxial DFB Laser Diode*, Emcore Corporation, August 2011, Data Sheet. [Online]. Available: http://www.emcore.com/assets/fiber/1933F-R-W_datasheet_2010.12.12.pdf

[21] I. Cox, C.H., E. Ackerman, G. Betts, and J. Prince, "Limits on the performance of rf-over-fiber links and their impact on device design," *Microwave Theory and Techniques, IEEE Transactions on*, vol. 54, no. 2, pp. 906 – 920, feb. 2006.

[22] *Fundamentals of RF and Microwave Noise Figure Measurements*, Agilent Technologies, Inc., May 2010, Application Note 57-1. [Online]. Available: http://cp.literature.agilent.com/litweb/pdf/5952-8255E.pdf

[23] *Microcoaxial RF, 50 Ohm, PCB Vertical Jack Receptacle, SMT, 1.25mm (.049) Mounted Height*, Molex, November 2011, Data Sheet. [Online]. Available: http://www.molex.com/webdocs/datasheets/pdf/en-us/0734120110_RF_COAX_CONNECTORS.pdf

[24] *MGA-86563, 0.5 6 GHz Low Noise, GaAs MMIC Amplifier*, Avago Technologies, August 2011, Data Sheet. [Online]. Available: http://www.avagotech.com/docs/AV02-2514EN

[25] *HMC849LP4CE, High Isolation SPDT Non-Reflective Switch SMT, DC - 6 GHz*, Hittite Microwave Corporation, August 2011, Data Sheet. [Online]. Available: http://www.hittite.com/products/view.html/view/HMC849LP4CE

[26] Mathworks. (2011, August) Matlab help pages @ONLINE. [Online]. Available: http://www.mathworks.se/help/toolbox/stats/boxplot.html

[27] *UTiFLEX*, Micro-Coax, Inc., 2010, Data Sheet. [Online]. Available: http://www.micro-coax.com/pages/technicalinfo/pdfs/UFB293C.pdf

[28] ANSI/TIA, "Optical fiber cabling components standard," TELECOMMUNICATIONS INDUSTRY ASSOCIATION, Tech. Rep. TIA/EIA-568-B.3, April 2000.

[29] *Fiber Optic Cable Assemblies - Specifications and Distribution*, Molex Interconnect, 2011, Data Sheet. [Online]. Available: http://rhu004.sma-promail.com/SQLImages/kelmscott/Molex/PDF_Images/987650-6401.pdf

[30] "The expression of uncertainty and confidence in measurement," United Kingdom Accreditation Service, Tech. Rep. UKAS publication M 3003, December 1997.

[31] R. Vaughan and J. Andersen, "Antenna diversity in mobile communications," *Vehicular Technology, IEEE Transactions on*, vol. 36, no. 4, pp. 149 – 172, nov. 1987.

[32] J. Ø. Nielsen and G. Pedersen, "Mobile handset performance evaluation using radiation pattern measurements," *Antennas and Propagation, IEEE Transactions on*, vol. 54, no. 7, pp. 2154 – 2165, july 2006.

Boyan Yanakiev received a bachelors degree in physics from Sofia University, Bulgaria in 2006 and a master's degree in Wireless Communication and a PhD degree from Aalborg University, Denmark in 2008 and 2011 respectively. His current position is as an antenna design engineer at Molex Antenna Business Unit and an industrial postdoctoral fellow at Aalborg University. His primary interests are in the area of small integrated mobile antennas, optical antenna measurement techniques and radio channel measurements. He has been involved in the design and development of multiple RF-to-optical convertors, for onboard handset measurements.

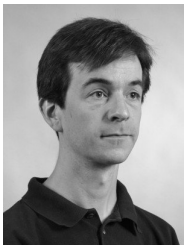

Jesper Ødum Nielsen received his master's degree in electronics engineering in 1994 and a PhD degree in 1997, both from Aalborg University, Denmark. He is currently employed at Department of Electronic Systems at Aalborg University where main areas of interests are experimental investigation of the mobile radio channel and the influence mobile device users have on the channel. He has been involved in MIMO channel sounding and modeling, as well as measurements using live GSM and LTE networks. In addition he has been working with radio performance evaluation, including over the air testing of active wireless devices.

Morten Christensen was born in 1973. He received the M.Sc. degree in Electrical Engineering from Aalborg University, Denmark in 1998. In 1998, he joined Bosch Telecom A/S, Pandrup, Denmark (acquired by Siemens Mobile Phones in 2000), where he designed integrated antennas for mobile terminals. In 2006 he joined Motorola A/S, Mobile Devices Aalborg where he was heading the EMC and Antenna department. He is now with Molex Antenna Business Unit responsible for the RF Research activities. His areas of interests includes handset antenna design, performance evaluation methods and radio propagation models.

Gert Frølund Pedersen was born in 1965 and married to Henriette and have 7 children. He received the B.Sc. E. E. degree, with honour, in electrical engineering from College of Technology in Dublin, Ireland, and the M.Sc. E. E. degree and Ph. D. from Aalborg University in 1993 and 2003. He has been employed by Aalborg University since 1993 where he is now full Professor heading the Antenna, Propagation and Networking group and is also the head of the doctoral school on wireless which some 100 phd students enrolled. His research has focused on radio communication for mobile terminals especially small Antennas, Diversity systems, Propagation and Biological effects and he has published more than 75 peer reviewed papers and holds 20 patents. He has also worked as consultant for developments of more than 100 antennas for mobile terminals including the first internal antenna for mobile phones in 1994 with lowest SAR, first internal triple-band antenna in 1998 with low SAR and high TRP and TIS, and lately various multi antenna systems rated as the most efficient on the market. He has been one of the pioneers in establishing over-the-air measurement systems. The measurement technique is now well established for mobile terminals with single antennas and he was chairing the COST2100 SWG2.2 group with liaison to 3GPP for over-the-air test of MIMO terminals.